

Supporting Information

for

**Molecular Investigations of the Prenucleation Mechanism of Bone-like Apatite Assisted by
Type I Collagen Nanofibrils: Insights into Intrafibrillar Mineralization**

Zhiyu Xue, Xin Wang and Dingguo Xu*

MOE Key Laboratory of Green Chemistry and Technology, College of Chemistry, Sichuan
University, Chengdu, Sichuan, 610064 PR China

* To whom correspondence should be addressed: dgxu@scu.edu.cn (D.X), Tel: 86-28-85406156.

Contents

Supporting Information	I
Figure S1. Definition of the bending angle in the collagen fibril structure.....	S1
Figure S2. The kink angle of collagen fibrils during the 300ns molecular dynamics relaxation.	S2
Figure S3. Ramachandran diagram for the collagen fibril structure.	S3
Figure S4. Distribution of the hydrogen bond density in the collagen fibril model. (A) for H-bonds within the single collagen fibrils, (B) for H-bonds between the collagen fibrils	S4
Figure S5. Evolution along the dynamic time course for the whole collagen fibril model.....	S5
Figure S6. Evolution along the dynamic time course for the Ca^{2+} and HPO_4^{2-} ions present in the isolated collagen model environment.....	S6
Figure S7. (A) Snapshot of the collagen prenucleation process of the one more replica calculation after 30 ns. (B) Cluster size distributions for the collagen fibrils. (C) Evolution of the nucleation probability for the Glu-Arg, Asp-Lys, Glu-Asp, and Lys-Arg pairs.....	S7
Figure S8. Cluster density distribution in the 67 nm D-periodicity of the one more replica calculation of collagen microfibrils (black line for calculated value, red line for experimental value).....	S8
Figure S9. Evolution along the dynamic time course (0, 2, 4, 8, 10, 20, and 30 ns) for the Ca^{2+} and HPO_4^{2-} ions that belong to the clusters formed in the gap region of the a–e band collagen fibrils. The a-bands are colored silver, while the while e-bands are colored yellow.	S9
Figure S10. Snapshot of the collagen fibrils in an aqueous solution of the $\text{HPO}_4^{2-}/\text{PO}_4^{3-}$ ions after 30 ns of molecular dynamics simulations.....	S10
Figure S11. Proportions of the various amino acids present in human type I collagen.	S11
Figure S12. (A) Snapshot of the collagen prenucleation process with the pure PO_4^{3-} after 30 ns. (B) The stoichiometry of two biggest clusters are $[\text{Posner}]_{\sim 57}$ for $\text{Ca}_{519}(\text{PO}_4)_{353}(\text{OH})_{57}$ and $[\text{Posner}]_{\sim 45}$ for $\text{Ca}_{401}(\text{PO}_4)_{271}(\text{OH})_{23}$ respectively.	S12
Figure S13. The view of arrangement of collagen fibrillar structure from the gap region.	S13
Table S1. Definitions of the models obtained using a combination of various anions in the solution phase. The corresponding ion concentrations are provided for each model	S14
Table S2. All types and proportions of the H-bonds within the single collagen fibrils	S15
Table S3. All types and proportions of the H-bonds between the collagen fibrils.....	S16

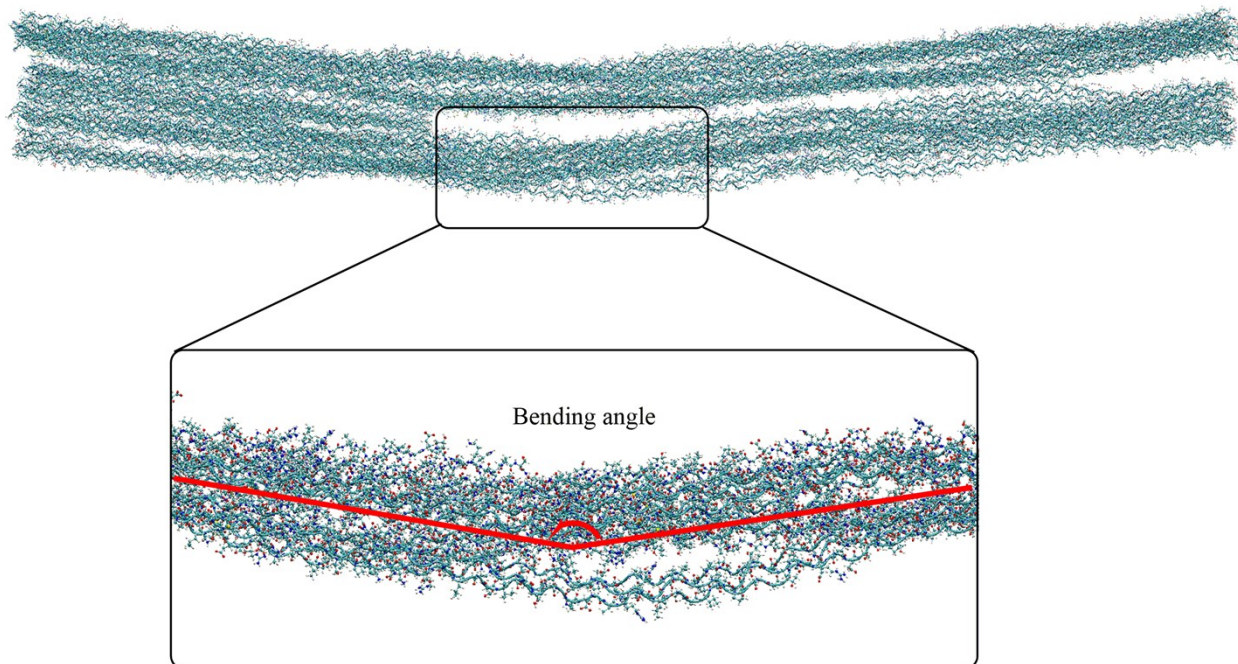


Figure S1. Definition of the bending angle in the collagen fibril structure.

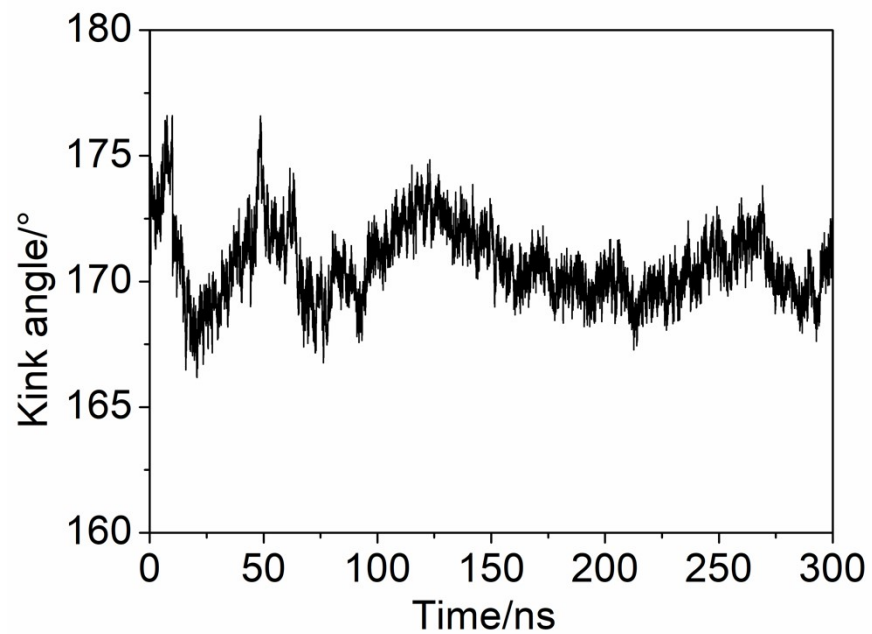


Figure S2. The kink angle of collagen fibrils during the 300ns molecular dynamics relaxation.

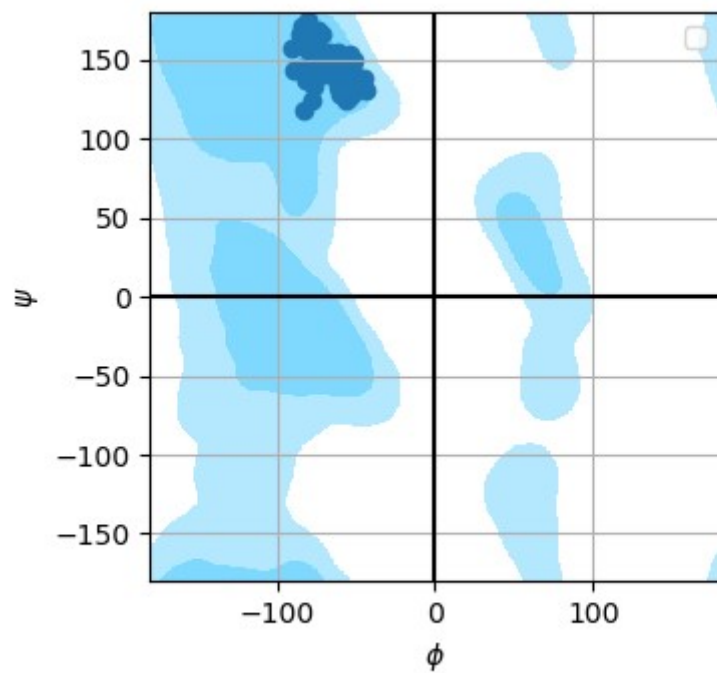


Figure S3. Ramachandran diagram for the collagen fibril structure.

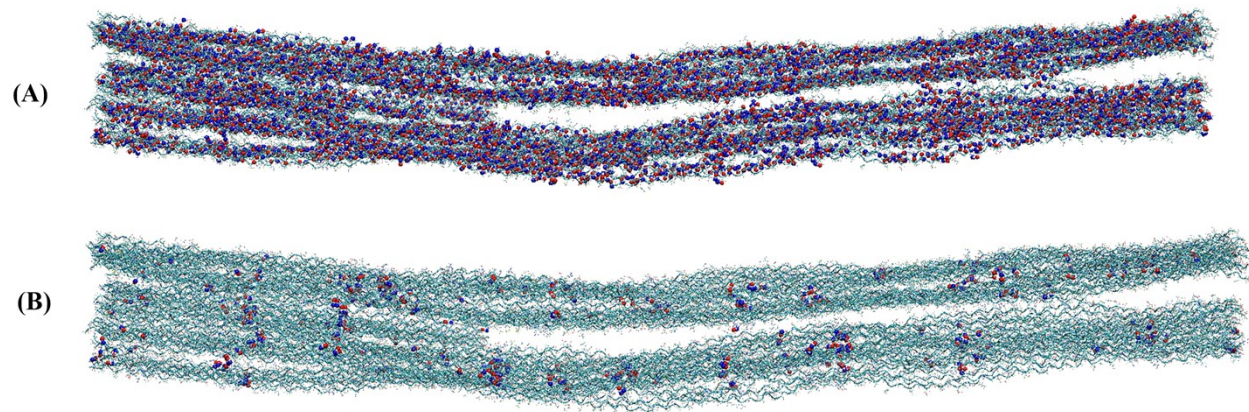


Figure S4. Distribution of the hydrogen bond density in the collagen fibril model. (A) for H-bonds within the single collagen fibrils, (B) for H-bonds between the collagen fibrils

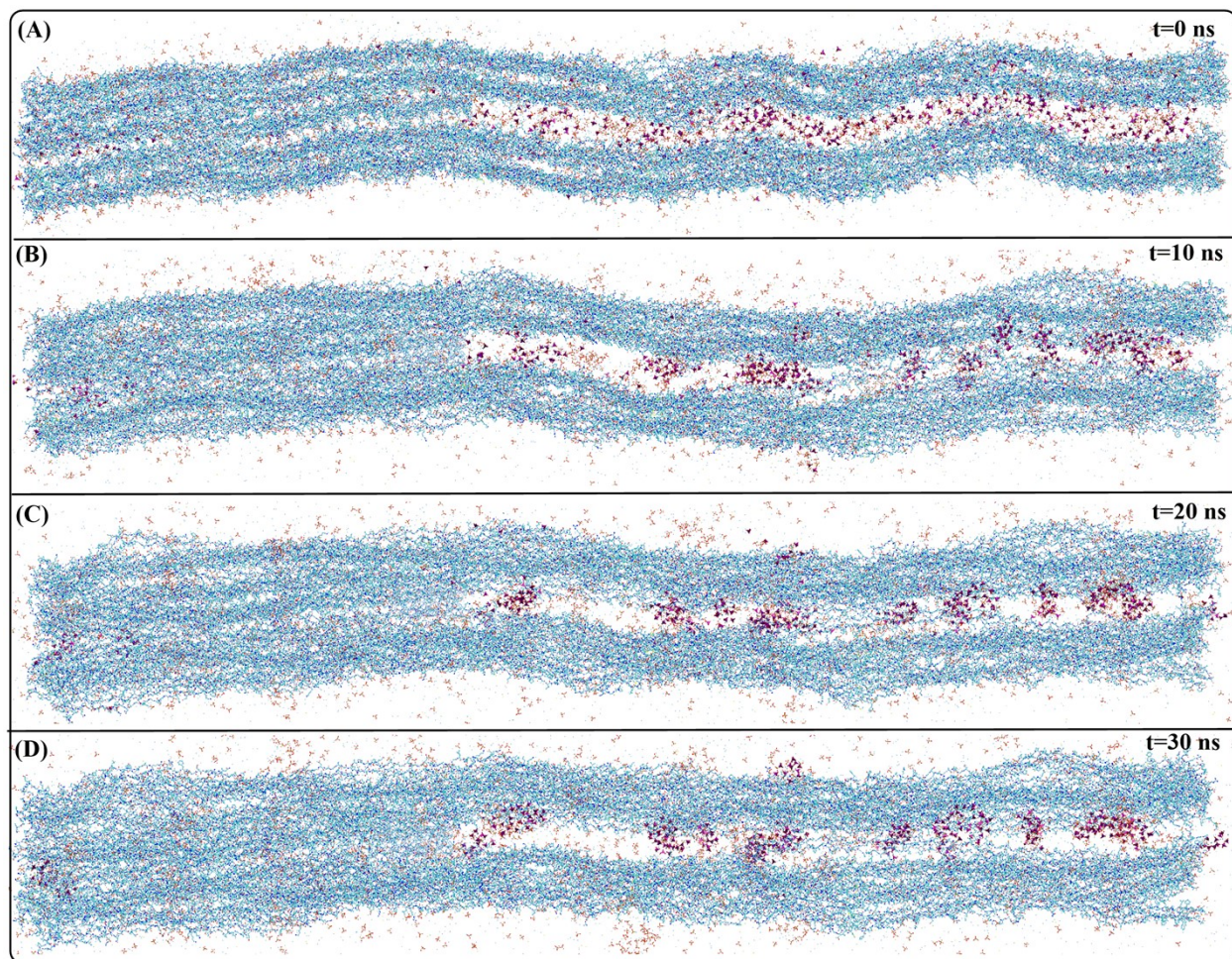


Figure S5. Evolution along the dynamic time course for the whole collagen fibril model.

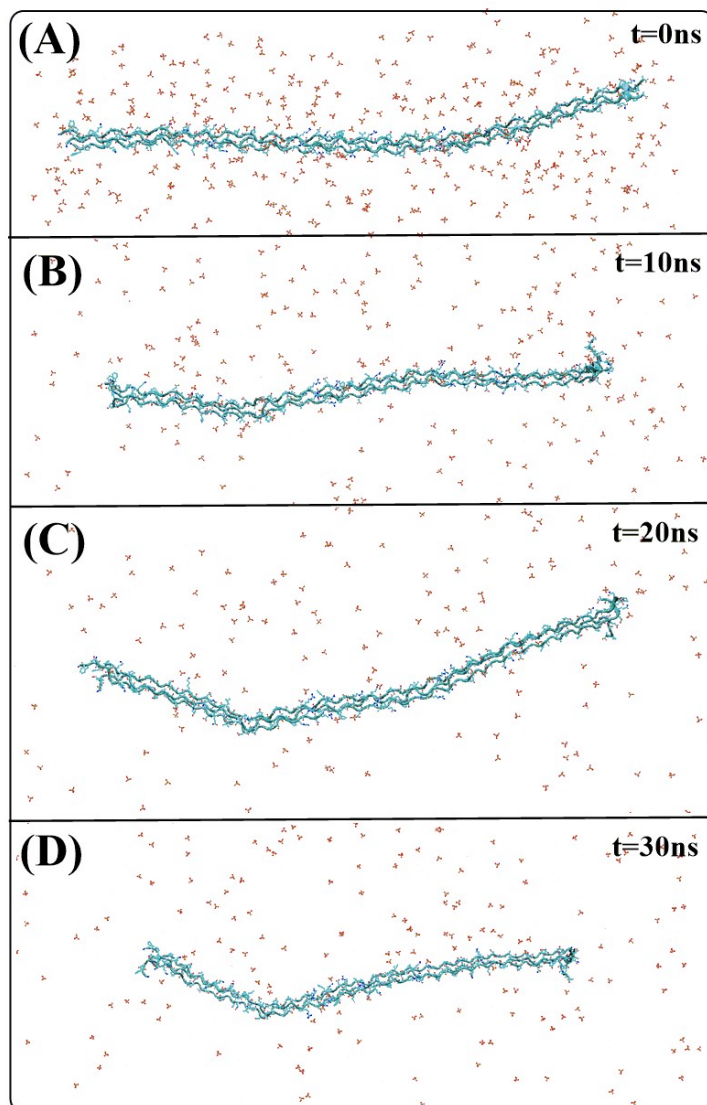


Figure S6. Evolution along the dynamic time course for the Ca^{2+} and HPO_4^{2-} ions present in the isolated collagen model environment.

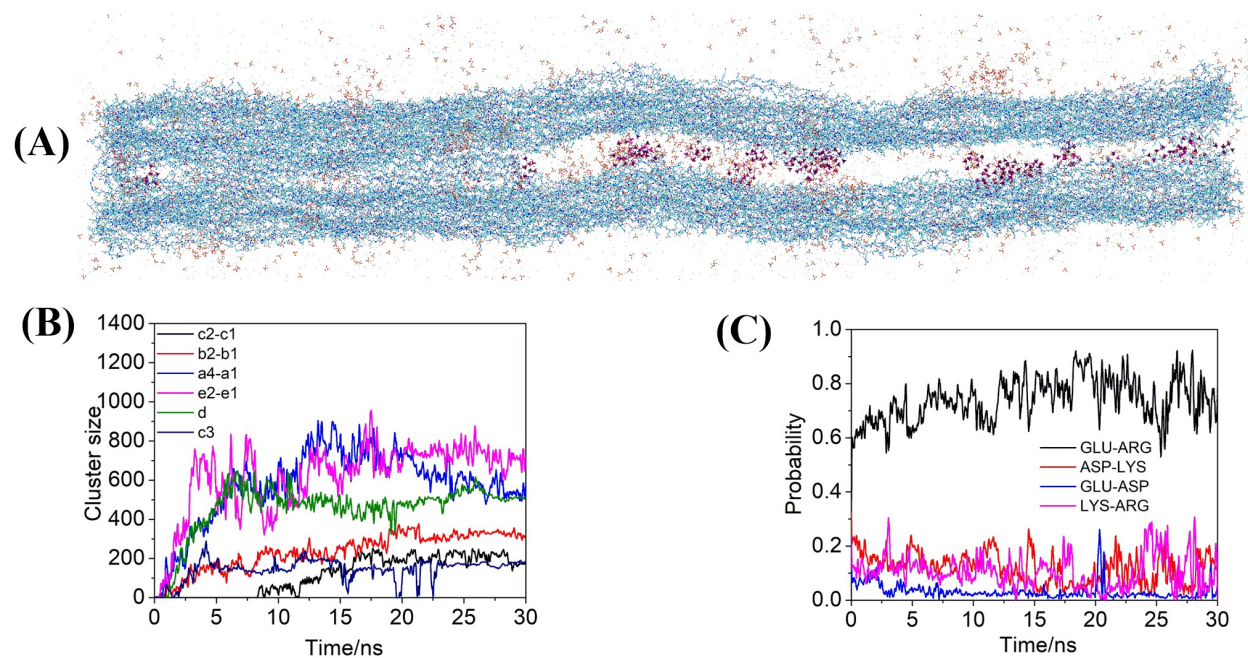


Figure S7. (A) Snapshot of the collagen prenucleation process of the one more replica calculation after 30 ns. (B) Cluster size distributions for the collagen fibrils. (C) Evolution of the nucleation probability for the Glu-Arg, Asp-Lys, Glu-Asp, and Lys-Arg pairs.

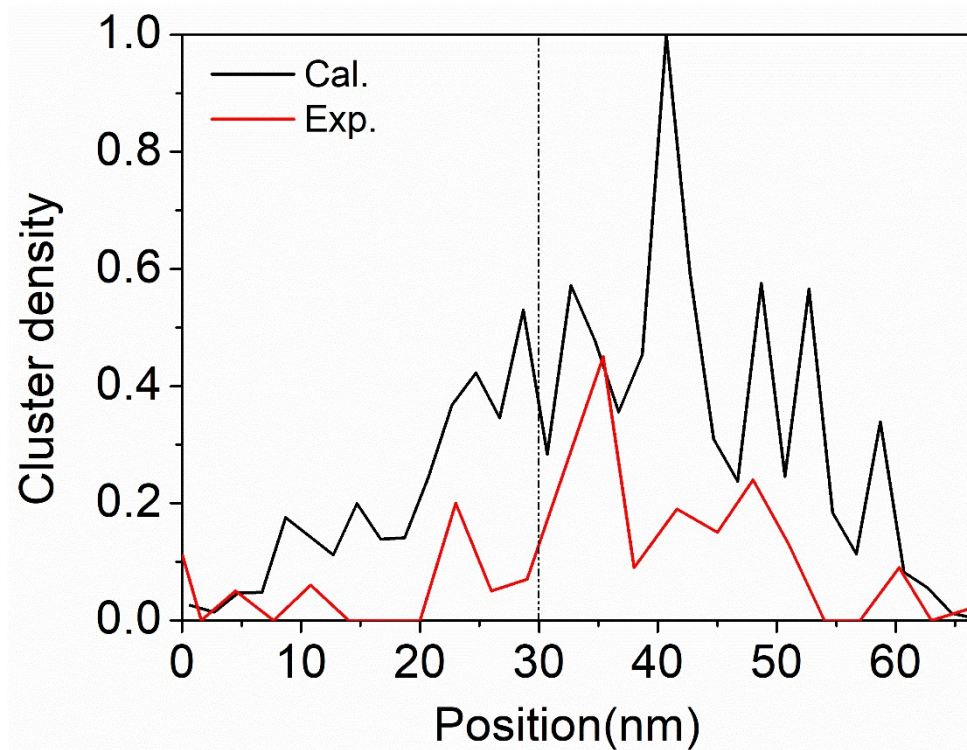


Figure S8. Cluster density distribution in the 67 nm D-periodicity of the one more replica calculation of collagen microfibrils (black line for calculated value, red line for experimental value).

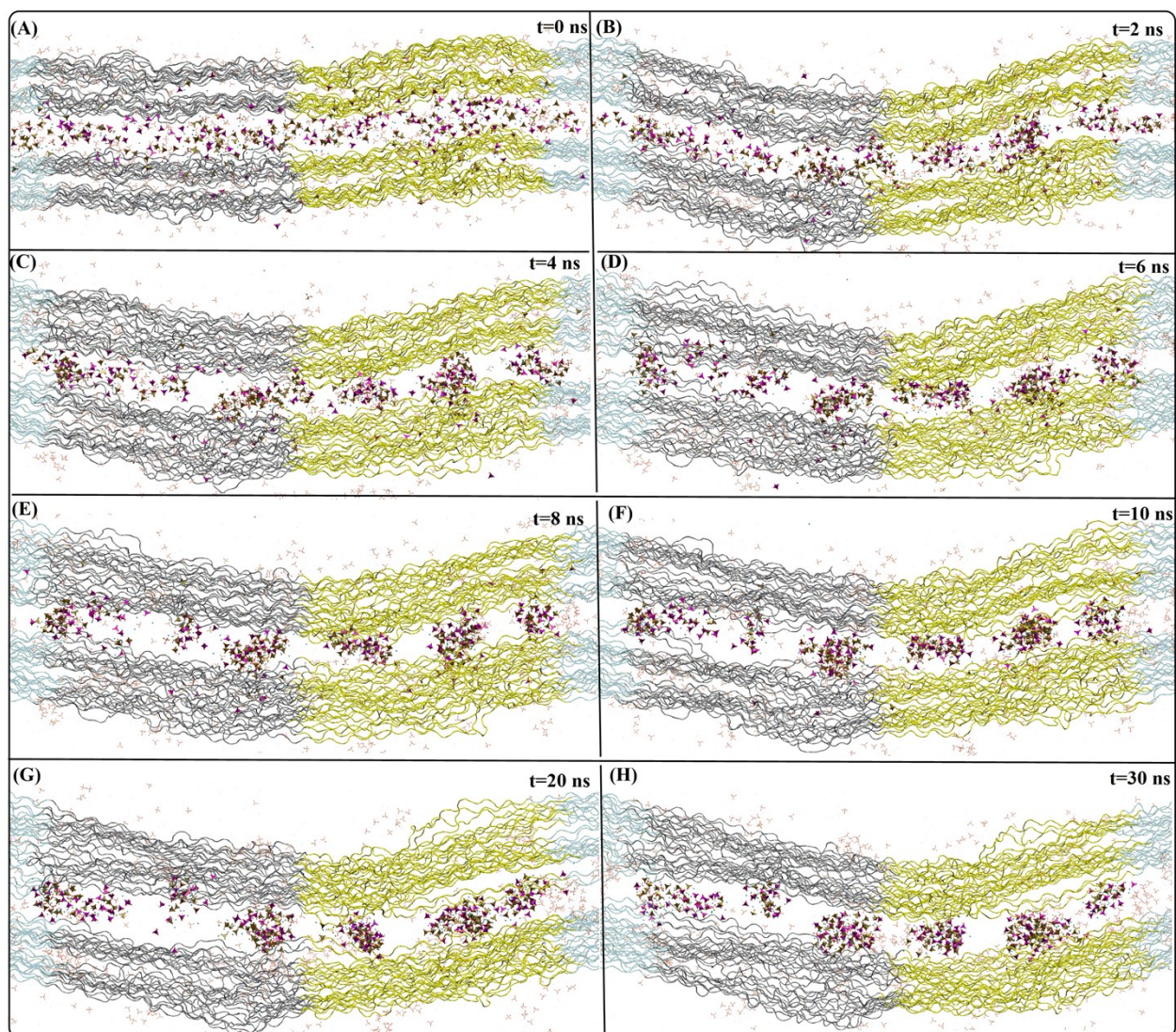


Figure S9. Evolution along the dynamic time course (0, 2, 4, 8, 10, 20, and 30 ns) for the Ca^{2+} and HPO_4^{2-} ions that belong to the clusters formed in the gap region of the a–e band collagen fibrils. The a-bands are colored silver, while the while e-bands are colored yellow.

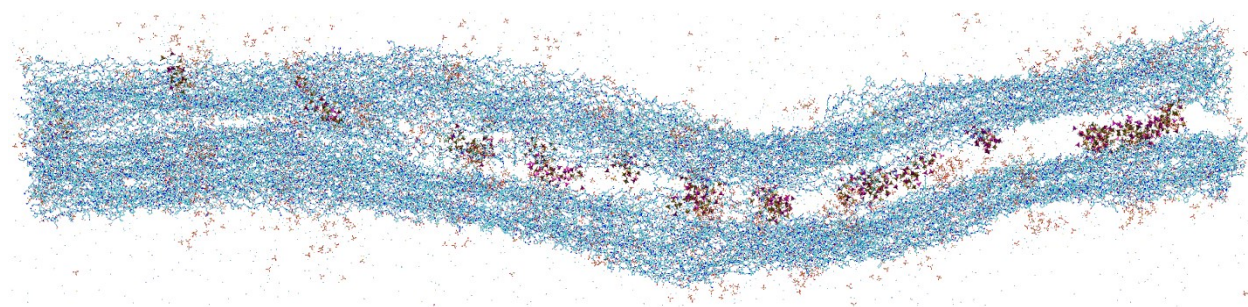


Figure S10. Snapshot of the collagen fibrils in an aqueous solution of the $\text{HPO}_4^{2-}/\text{PO}_4^{3-}$ ions after 30 ns of molecular dynamics simulations.

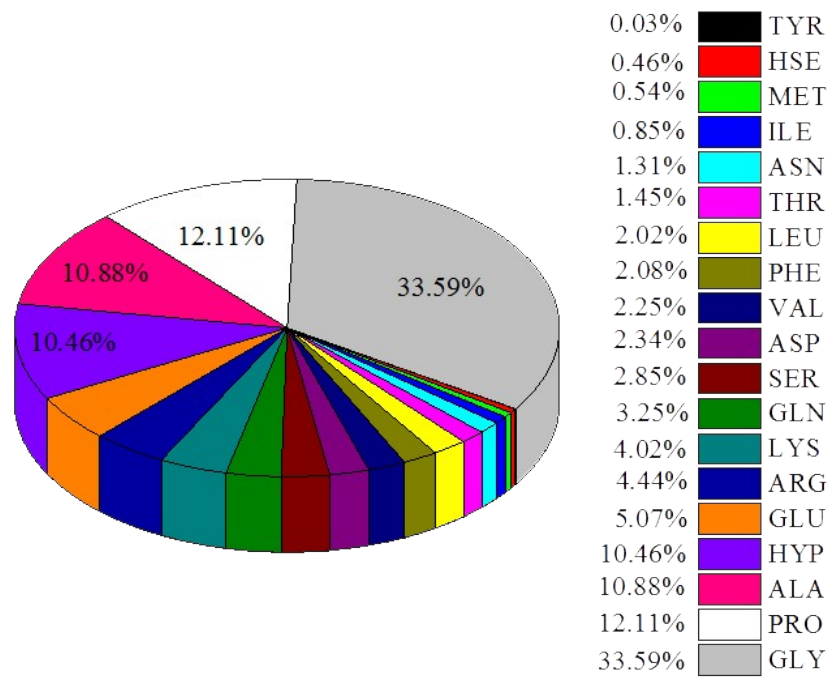


Figure S11. Proportions of the various amino acids present in human type I collagen.

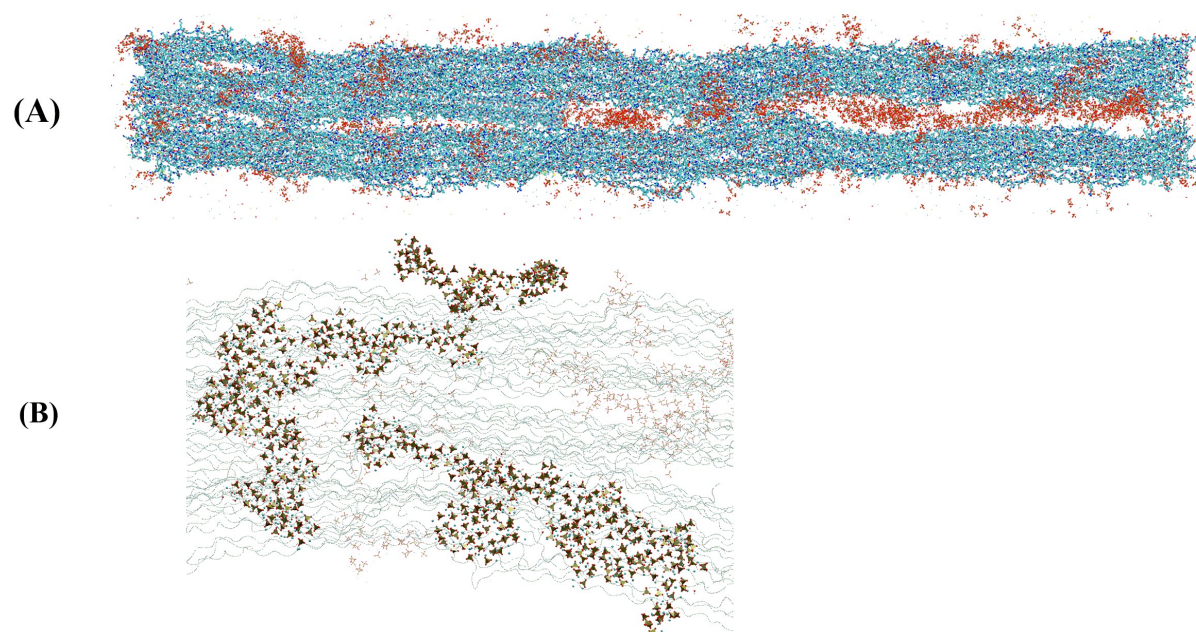


Figure S12. (A) Snapshot of the collagen prenucleation process with the pure PO_4^{3-} after 30 ns. (B) The stoichiometries of two biggest clusters are $[\text{Posner}]_{-57}$ for $\text{Ca}_{519}(\text{PO}_4)_{353}(\text{OH})_{57}$ and $[\text{Posner}]_{-45}$ for $\text{Ca}_{401}(\text{PO}_4)_{271}(\text{OH})_{23}$ respectively.

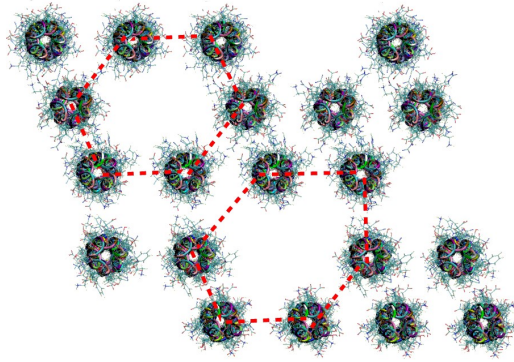


Figure S13. The view of arrangement of collagen fibrillar structure from the gap region.

Table S1. Definitions of the models obtained using a combination of various anions in the solution phase. The corresponding ion concentrations are provided for each model

Anion composition	Concentration (M)				
	$C_{Ca^{2+}}$	$C_{HPO_4^{2-}}$	$C_{PO_4^{3-}}$	C_{Na^+}	C_{Cl^-}
HPO_4^{2-}	0.7	0.42	-	0.1	0.66
$HPO_4^{2-} + PO_4^{3-}$	0.7	0.21	0.21	0.1	0.45

Table S2. All types and proportions of the H-bonds within the single collagen fibrils

GLY:N---PRO:O	0.238347	LEU:N---HYP:O	0.001887	ASN:N---ALA:O	0.000377
GLY:N---ALA:O	0.132289	GLN:N---ALA:O	0.001887	GLN:N---LEU:O	0.000377
GLY:N---GLU:O	0.10568	ALA:N---HYP:O	0.001698	GLU:N---GLY:O	0.000377
GLY:N---LEU:O	0.051519	LYS:N---ILE:O	0.001698	SER:O---PRO:O	0.000189
ARG:N---ARG:O	0.050009	GLU:N---ASN:O	0.001698	HIS:N---HIS:N	0.000189
GLY:N---SER:O	0.037743	LYS:N---ARG:O	0.00151	VAL:N---GLU:O	0.000189
GLY:N---ASP:O	0.031515	GLN:N---ASP:O	0.00151	THR:O---GLY:O	0.000189
GLY:N---LYS:O	0.027175	GLU:N---GLU:O	0.001321	SER:N---ASP:O	0.000189
GLY:N---PHE:O	0.024344	LYS:N---SER:O	0.001321	ASN:N---HIS:N	0.000189
GLY:N---VAL:O	0.024156	ARG:N---THR:O	0.001132	SER:N---GLY:O	0.000189
LYS:N---GLU:O	0.02208	GLN:N---GLU:O	0.001132	VAL:N---HYP:O	0.000189
ARG:N---GLU:O	0.021702	THR:N---GLU:O	0.001132	GLN:N---HIS:N	0.000189
GLY:N---ARG:O	0.019815	ALA:N---ASP:O	0.001132	SER:N---ASN:O	0.000189
ARG:N---ASP:O	0.018117	GLY:N---TYR:O	0.000944	GLY:N---HYP:O	0.000189
GLY:N---ASN:O	0.017928	LYS:N---ALA:O	0.000944	VAL:N---PRO:O	0.000189
LYS:N---ASP:O	0.016984	SER:N---GLU:O	0.000944	SER:O---HYP:O	0.000189
GLY:N---GLN:O	0.015097	GLN:N---ARG:O	0.000944	SER:N---HIS:N	0.000189
ARG:N---HYP:O	0.012833	ARG:N---LEU:O	0.000944	LEU:N---VAL:O	0.000189
GLY:N---ILE:O	0.011512	LEU:N---ASP:O	0.000755	ASP:N---HYP:O	0.000189
GLN:N---GLN:O	0.009624	PHE:N---HYP:O	0.000755	GLY:N---HIS:N	0.000189
GLY:N---HIS:O	0.009436	ARG:N---PRO:O	0.000566	THR:N---HYP:O	0.000189
GLY:N---THR:O	0.007926	ASN:N---HYP:O	0.000566	ASN:N---GLY:O	0.000189
ARG:N---LYS:O	0.005473	LEU:N---ASN:O	0.000566	THR:O---HYP:O	0.000189
ARG:N---ALA:O	0.005095	GLN:N---THR:O	0.000566	LYS:N---GLY:O	0.000189
GLY:N---GLY:O	0.004718	LYS:N---GLN:O	0.000566	SER:O---ALA:O	0.000189
ARG:N---SER:O	0.00434	ASN:N---SER:O	0.000377		
ASN:N---ASP:O	0.004152	THR:N---ASN:O	0.000377		
LYS:N---LYS:O	0.003963	SER:O---GLU:O	0.000377		
GLY:N---MET:O	0.003774	ALA:N---ASN:O	0.000377		
LYS:N---HYP:O	0.003586	HIS:N---ASN:O	0.000377		
ARG:N---VAL:O	0.003397	ASN:N---GLU:O	0.000377		
GLN:N---HYP:O	0.002831	ALA:N---GLU:O	0.000377		
ARG:N---GLN:O	0.002642	HYP:O---GLU:O	0.000377		
GLU:N---HYP:O	0.002642	SER:O---GLY:O	0.000377		
ARG:N---ASN:O	0.002453	GLN:N---HIS:O	0.000377		
ARG:N---GLY:O	0.002453	LYS:N---THR:O	0.000377		
LYS:N---ASN:O	0.002265	ASP:N---ASN:O	0.000377		
SER:N---HYP:O	0.002076	ASP:N---ASP:O	0.000377		

Table S3. All types and proportions of the H-bonds between the collagen fibrils

ARG:N---GLU:O	0.3882682	LYS:N---GLY:O	0.0027933
LYS:N---GLU:O	0.1480447	ARG:N---ASN:O	0.0027933
ARG:N---ASP:O	0.1480447	VAL:N---GLN:O	0.0027933
ARG:N---GLY:O	0.0446927	THR:N---ASP:O	0.0027933
LYS:N---ASP:O	0.0391061	ARG:N---ALA:O	0.0027933
ARG:N---HYP:O	0.0251397	ASN:N---ARG:O	0.0027933
SER:N---GLU:O	0.0223464	SER:N---GLN:O	0.0027933
GLN:N---HYP:O	0.0195531	ARG:N---VAL:O	0.0027933
GLN:N---GLY:O	0.0111732	THR:N---GLU:O	0.0027933
GLY:N---GLU:O	0.0083799	ASN:N---ASN:O	0.0027933
ASN:N---HYP:O	0.0083799	THR:N---PRO:O	0.0027933
HYP:N---GLY:O	0.0083799	HIS:N---GLY:O	0.0027933
LYS:N---HYP:O	0.0055866	ALA:N---ASN:O	0.0027933
ALA:N---GLN:O	0.0055866	ALA:N---HYP:O	0.0027933
MET:N---HYP:O	0.0055866	SER:N---GLY:O	0.0027933
ALA:N---GLY:O	0.0055866	SER:N---HYP:O	0.0027933
ALA:N---SER:O	0.0055866	ARG:N---ILE:O	0.0027933
SER:N---ASP:O	0.0055866	ILE:N---HYP:O	0.0027933
LYS:N---ASN:O	0.0055866		
VAL:N---ASN:O	0.0027933		
ASP:N---HYP:O	0.0027933		
ARG:N---SER:O	0.0027933		
GLN:N---GLU:O	0.0027933		
GLN:N---SER:O	0.0027933		
HYP:N---ASP:O	0.0027933		
GLN:N---ARG:O	0.0027933		
THR:N---HYP:O	0.0027933		
ASP:N---GLU:O	0.0027933		
GLN:N---GLN:O	0.0027933		
HIS:N---GLU:O	0.0027933		
LYS:N---GLN:O	0.0027933		
ASN:N---GLU:O	0.0027933		
ASN:N---GLY:O	0.0027933		